Available online at www.sciencedirect.com
ScienceDirect
Journal of the European Ceramic Society 30 (2010) 1177–1185
www.elsevier.com/locate/jeurceramsoc

Fabrication of particle and composition gradients by systematic interaction of sedimentation and electrical field in electrophoretic deposition

Sylvia Bonnas [a,b,*], Hans-Joachim Ritzhaupt-Kleissl [b], Jürgen Haußelt [a,b]

[a] *Laboratory for Materials Processing, Department of Microsystems Engineering (IMTEK), University of Freiburg, D-79110 Freiburg, Germany*
[b] *Institute for Materials Research III, Forschungszentrum Karlsruhe, D-76021 Karlsruhe, Germany*

Available online 11 September 2009

Abstract

The systematic interaction of sedimentation and electrical field in electrophoretic deposition allows the tailoring of specific properties of deposited green bodies. This technique permits a selective deposition of the nanosized fraction of conventional powders with broad or non-monomodal particle size distribution, thus making preceding classification obsolete. Potential applications are coatings with a very smooth surface or the replication of microstructures or moulds which are filled with nanosized particles and subsequently with coarser particles as support in one process step. Also, graded structures can be fabricated with regard to particle size distribution, porosity and composition (e.g. zirconia toughened alumina). In this paper, the interaction of sedimentation and electrical field in electrophoretic deposition is described. In addition the effectiveness of the combined process will be shown.

Keywords: Electrophoretic deposition; Suspension; Al_2O_3; ZrO_2; Calcination

1. Introduction

In microsystem technology and microchemical engineering, the application of submicron and nanosized ceramic particles is gaining importance because of the required smooth surfaces and dimensional accuracy. In conventional shaping techniques like axial pressing, slip casting or microinjection moulding nanosized powders are difficult to apply. For these powders, electrophoretic deposition (EPD) is a more suitable method,[1,2] because the deposition rate is independent of particle size as long as EPD is carried out perpendicular to sedimentation.

Electrophoretic deposition is a colloidal processing technique first observed in 1808 by the Russian scientist Reuss,[3] the first description of the deposited yield was made in 1940 by Hamaker.[4]

Electrophoretic deposition is achieved via motion of charged particles in a fluid medium under the influence of an electric field towards an oppositely charged electrode and the formation of a stable deposit on the electrode[1,5–8] or on a membrane.[6,9] Homogeneous deposits with a high mechanical strength and a low surface roughness can only be obtained by using well dispersed suspensions.[10] EPD is used for many applications, such as for the manufacturing of coatings, microstructures, laminated or graded materials or for infiltration of porous materials.[5–7,9,11] A wide range of materials and combinations can be employed.[1,10,12]

For various applications, like biomaterials, joining of ceramics to metals, thermal shielding and optical/electronical functions, functionally graded materials (FGM) are advantageous.[13] They permit joining of materials with different thermomechanical or physical properties. For example, by a systematic choice of the materials employed thermal protective coatings or a continuous changeover between electrical insulating and conductive materials can be made. Different techniques to produce such FGMs have been tested successfully, like thermal and plasma spraying, powder processing, chemical and physical vapour deposition, electrochemical processing and filtration, microwave processing and field activated synthesis. However, not all these techniques render a continuously graded morphology. Furthermore, many of these techniques are time consuming and expensive.[8,9,14]

The double-step electrophoretic deposition is a promising technique to make layered composites. It is a simple and cost-effective method with high deposition rates. Layered composites

* Corresponding author at: Laboratory for Materials Processing, Department of Microsystems Engineering (IMTEK), University of Freiburg, D-79110 Freiburg, Germany.
E-mail addresses: sylvia.bonnas@web.de (S. Bonnas), hans-joachim.ritzhaupt-kleissl@imf.fzk.de (H.-J. Ritzhaupt-Kleissl), juergen.hausselt@imf.fzk.de (J. Haußelt).

0955-2219/$ – see front matter © 2009 Elsevier Ltd. All rights reserved.
doi:10.1016/j.jeurceramsoc.2009.08.007

can be obtained by alternating electrophoretic deposition of suspensions containing different materials.[14–16] A continuous concentration gradient, however, requires a different processing route where a suspension containing a second constituent is continuously added to a circulating suspension with the first constituent.[7,8,17] The colloidal properties of the different materials may result in different deposition behaviours due to different zeta potentials. Also coagulation or segregation in the suspension can occur. Without solving these problems, a perfectly continuous gradient cannot be obtained. Complex calculations and an exact control of process parameters are necessary to predict and tailor the gradient in the deposit.

Another production method for functionally graded materials is the electrophoretic impregnation (EPI). Via EPI a green body with open porosity is impregnated with nanosized particles with the steepness of the gradient depending on the porosity of the matrix, the particle size/pore size ratio, the viscosity and the zeta potential of the nanosized particle suspension and the applied electrical field strength.[9] The amount of the secondary phase within the composite, however, is limited by the porosity of the matrix shaped in a first process step. Furthermore, the thickness of the graded layers is limited to a range of approximately 20 μm to several mm.

For realising continuously functional graded materials, the systematic interaction of sedimentation and electrical field in electrophoretic deposition (S-EPD) is a suitable method. Simultaneously with electrophoretic deposition, sedimentation occurs depending on diameter and density of the particles and on the solids content of the suspension.[18] By using S-EPD, the particle size distribution of the deposited green body can be changed gradually. If, for example, the gravitational force acting on particles of a critical diameter is compensated by the force due to the applied electrical field, these particles remain motionless,[19] whereas smaller particles will be deposited.

S-EPD can be used for producing coatings or microstructures with a very smooth surface by depositing only the nanosized fraction of a conventional powder with broad or non-monomodal particle size distribution; thus, no preceding classification is necessary and no expensive nanosized powders have to be used. After the microstructured moulds have been filled with the nanofraction of a powder a strong support of bigger particles is deposited subsequently by increasing the applied electrical field strength. The process can be used for shaping components with continuous gradients in density or particle size across the layer thickness, as well as for compositional gradients.

For a better process control and the manufacturing of components with predictable gradients, kinetics of S-EPD have to be known, which is the main goal of this work. First of all a mathematical description of the kinetics of EPD is necessary.

In 1940 Hamaker proposed an equation to calculate the yield in electrophoretic deposition[4] which can be written as follows:

$$\frac{dm}{dt} = a \cdot c \cdot \frac{\varepsilon_0 \cdot \varepsilon_r \cdot \zeta \cdot f}{\eta} \cdot E \cdot A \tag{1}$$

this equation describes the quantity of particles reaching the electrode (in most cases a is assumed to be close to 1), c is the particle concentration, $\varepsilon_0 \bullet \varepsilon_r$ is the permittivity, ζ is the zeta-potential, f is the related correction factor, η is the viscosity of the suspension medium, E is the applied electric field strength, A is the surface area of the electrodes and t is the deposition time.

In 1962 Avgustinik developed a similar equation to calculate deposition yield for a cylindrical geometry[20] and upgraded it in 1967 by factoring the decreasing particle concentration within the suspension due to electrophoretic deposition into this equation.[21]

Based on Hamaker's equation, Biesheuvel developed a correction term incorporating the green body growth and therewith the shifting of the frontier between green body and suspension.[10]

It turned out that Hamaker's description of the deposited yield in case of EPD was only valid for short deposition times.[22] The decrease in particle concentration of the suspension due to electrophoretic deposition was neglected. Another approach to include the decrease was set up by Zhang in 1994[23]

$$m = m_0 \cdot (1 - e^{-k \cdot t}) \tag{2}$$

where the parameter k is represented by

$$k = a \cdot \frac{A}{V} \cdot \frac{\varepsilon_0 \cdot \varepsilon_r \cdot \zeta \cdot f}{\eta} \cdot E \tag{3}$$

The deposited mass m is a function of the initial mass m_0 in the electrophoretic cell, the parameter k and the deposition time t.

For a correct description of the interaction of sedimentation and electrical field in electrophoretic deposition the knowledge of the sedimentation behaviour of the dispersed particles is essential. The settling speed of an isolated particle in a diluted dispersion is described by the equation of Stokes [24]

$$v_S = \frac{2 \cdot g \cdot (\rho_P - \rho_F) \cdot r^2}{9 \cdot \eta} \tag{4}$$

The settling velocity depends on the acceleration of gravity g, the density of powder ρ_P, and medium ρ_F, the viscosity of the medium η and the particle radius r.

In 1951 Kynch published a review of the theory of sedimentation, in which he specified an equation obtained by Einstein and Smoluchowski, where the density of the particles is small and their mutual distance is much bigger than their size.[24] Another review of sedimentation was given by Bürger in 2001. He presented beside others the equation of Richardson and Zaki, where the batch-settling velocity of particles in real suspensions of small particles is described.[25]

When sedimentation and electrical field interact during EPD, the critical radius of particles remaining motionless can be calculated in a simple form by using the equations of Hamaker and Stokes. The critical radius r_{crit} can be varied by adjusting the electrical field strength and can be calculated as follows:

$$r_{crit} = \sqrt{\frac{9 \cdot \varepsilon_0 \cdot \varepsilon_r \cdot \zeta \cdot f}{2 \cdot g \cdot (\rho_P - \rho_F)} \cdot E} \tag{5}$$

The goal of this work is to investigate experimentally the kinetics of the so called S-EPD as a systematic interaction of sedimentation and electrophoretic deposition to allow the production of graded coatings with regard to particle size distribution and composition (Al_2O_3–ZrO_2).

2. Experimental

2.1. Experimental challenges

Several sources for discrepancies between simulation and experimental data in the results of this work have to be considered and will be mentioned in this subsection.

2.1.1. Powder characteristics

In all theoretical considerations and modelling assumptions powder particles are assumed as spherical. In reality they are irregular. This is also valid for the experiments performed here. So differences between measured and calculated sedimentation behaviour have to be accepted. According to their directional alignment irregular particles can settle down faster or slower than predicted by calculation.

2.1.2. Powder particle distribution

Theoretical considerations always consider monodisperse or multidisperse powder distributions. This is not the case in reality. Here always particle size distributions exist. To come close to theory generally powers with particle size distributions as narrow as possible were chosen for the experiments, but still discrepancies exist, i.e., when it is stated that a certain powder size is smaller than or larger than a certain limit, this is not exactly true. There always exists a certain quantity of particles smaller or larger than this value influencing the experimental results.

Furthermore real powders tend to agglomerate. To get the powders disagglomerated was one of the major challenges during experimental work. But even if the powders may be disagglomerated during characterizational measurements they may again re-agglomerate or still more disagglomerate during the deposition.

2.1.3. Sedimentation and EPD of powders from different materials and with different particle sizes

Another source of uncertainty exists when the combined effects of sedimentation and electrophoretic deposition of materials with different material densities are considered. So, regarding a coarse ZrO_2-powder with a theoretical density of about 6 g/cm^3 and a fine Al_2O_3-powder with a theoretical density of about 4 g/cm^3 at a given electric field strength, at first only Al_2O_3-particles up to a certain size should be deposited. But it cannot be excluded that also small ZrO_2-particles are deposited, which exist as small residue in the coarse powder. The same is valid for high field strengths, when all Al_2O_3-particles should have been deposited so that now the deposit should only show ZrO_2. But there may be some coarse Al_2O_3-particles originating from the coarse residue or from newly built agglomerates.

2.1.4. Characterization methods

Barreiros[26] showed that the measured values of particle size distribution depend on the measurement method. When particles are irregular; optical analysis methods result in larger particle sizes than given by the sedimentation method. This was also shown by Lehmann.[27] So results of particle size distribution have always to be considered regarding the measuring method and generally as estimation more or less narrow to reality.

Regarding energy dispersive X-ray analysis (EDX) as a characterization method for the Al- and Zr-distribution in the deposited layers, it must be considered that the electron beam has a real cross-sectional area of a few μm. So the distribution of the elements is not measured at a defined point but as an average across this area. Furthermore the placement of the electron beam at a predestined point of a very small cross-sectional area with high accuracy is very difficult if not impossible. These uncertainties also must be taken into consideration.

All these above mentioned sources of uncertainties must be kept in mind when the experimental results are compared to the theoretical considerations. So no 100% agreement between experiment and simulation can be expected. Nevertheless in principle the experimental results shall support the theoretical considerations.

2.2. Materials and suspensions

The following powders were used: (1) ZrO_2 Unitec – 10 μm with 5 wt.% Y_2O_3 (Unitec Ceramics, UK), with a d_{50} of 1.73 μm, (2) ZrO_2 Unitec – 1 μm with 5 wt.% Y_2O_3 (Unitec Ceramics, UK), with a d_{50} of 0.29 μm and (3) α-Al_2O_3 RC-LS (Baikowski-Malakoff Incorporated, USA), with a d_{50} of 1.3 μm.

Aqueous slurries of the powders were prepared with a solids content of 10 vol.%. As dispersant a commercial polyelectrolyte based on carbonic acid (Dolapix CE 64, Zschimmer & Schwarz, Germany) was used. Tetramethylammonium hydroxide (TMAH, Sigma–Aldrich, Germany) and hydrochloric acid (HCl, Merck, Germany) were used to adjust the pH and to stabilize the suspensions.

The slurries were prepared using a magnetic stirrer to suspend the powders in the solvent containing the dispersant. Dispersion of the particles and homogenisation of the suspension were carried out for 5 min in an ultrasonic bath and for 1 h at 200 min^{-1} in a planetary ball mill using zirconia balls and a grinding beaker (PM 400/2, Retsch, Germany). Afterwards, in case of the aqueous slurries, the pH value was adjusted with TMAH or HCl.

2.3. Characterisation of the suspensions

One key requirement for the investigation of the kinetics of EPD and S-EPD is the knowledge of the particles' zeta potential. It was measured by means of a ZetaSizer 3000 HAS (Malvern Instruments, UK), with diluted TMAH and HCl added for automatic titration.

The particle size distribution was measured using laser light diffraction particle size analyzer (LS 230, Coulter-Beckman, Germany). This allows measuring particle sizes from 0.04 μm to 2000 μm by combination of laser light scattering for measuring the coarse particles and polarization intensity differential scattering (PIDS) for measuring the finer particles. To determine sedimentation kinetics, sedimentation of particles was investigated in cylinders and by in situ measurements of the particle size distribution with the LS 230. This was executed by permitting particles to settle down in the sample chamber and continu-

ously measuring the particle size distribution remaining in the suspension each 15 min with a measurement duration of 60 s.

2.4. Electrophoretic deposition

For the S-EPD a glass beaker was used as EPD-cell. The working electrode was made of brass, the counter electrode of stainless steel in case of the aqueous suspensions. In case of non-aqueous suspensions, both electrodes were made of platinum coated silicon dies. The distance between the electrodes was 15 mm, when the electrodes were positioned horizontally.

The electrodes were weighed before and after electrophoretic deposition to determine the deposited mass.

3. Results and discussion

3.1. Zeta potential

Aqueous slurries of the coarse powders were prepared with different dispersant quantities using a powder concentration of 10 vol.%. For measurement of the zeta potential, the suspensions were diluted to a powder concentration of 2.5 ppm. Measurements were carried out in two steps: from neutral to acidic and from neutral to basic.

In Fig. 1 the zeta potential is shown as function of pH for ZrO_2 Unitec – 10 μm and Al_2O_3 RC-LS for a dispersant concentration (Dolapix CE 64) of 0.2 wt.%.

For the ZrO_2 Unitec – 10 μm, at pH 2.5 the zeta potential is 42 mV. At pH 5, the isoelectric point (IEP) is reached and the zeta potential decreases to −64 mV at pH 11.5. The Al_2O_3 RC-LS shows higher zeta potentials than the zirconia for pH < 6.5 (IEP). The zeta potential decreases from 65 mV at pH 2.5 to −63 mV at pH 11.5. From pH 9 to 11.5, the zeta potential of zirconia and alumina are nearly identical, which means that the resulting gradient in S-EPD of zirconia toughened alumina (ZTA) should only be controlled by the difference in density of ZrO_2 and Al_2O_3 and can thus be adjusted by changing the applied electrical field strength. This means that by S-EPD the fraction of the heavier zirconia particles can be varied across the thickness of the deposit without changing the slurry composition.

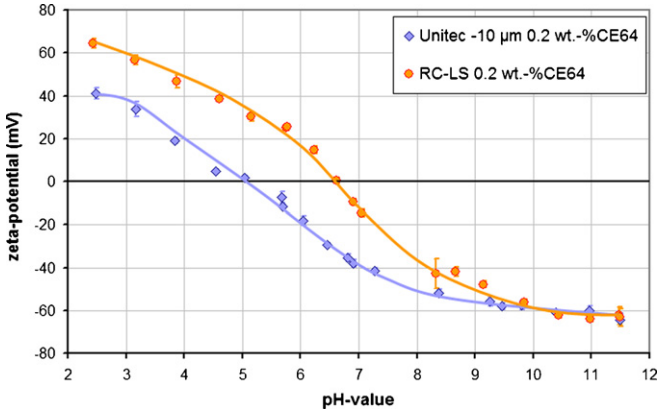

Fig. 1. Zeta potential as function of pH.

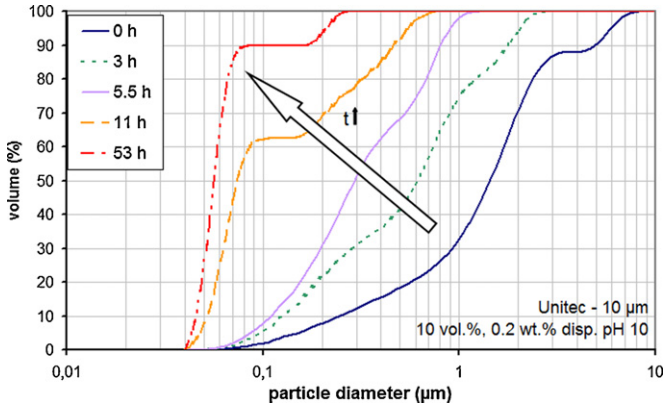

Fig. 2. In situ measurement of the particle size distribution.

3.2. Sedimentation kinetics

To determine sedimentation kinetics, 10 ml of the aqueous slurries were filled in cylinders. The movement of the sedimentation front was observed as a function of time. As reported previously[28,29] for the suspensions with optimised dispersant and at pH 10 a linear correlation of moving distance x of the particles and sedimentation time t was observed. This is an indication of a stable suspension.[30] As reported in literature, stable suspensions exhibit free sedimentation behaviour.[31] Thus, the assumption of isolated particle sedimentation is proved to be correct. Therefore, the description of sedimentation kinetics according to Stokes (Eq. (4)) is valid for the mathematical description of S-EPD for stabilised suspensions.

To allow determination of the sedimentation kinetics of the powders taking into account their real particle size distribution (PSD), in situ measurements were carried out. In Fig. 2 the sedimentation kinetics of an aqueous zirconia suspension stabilised with 0.2 wt.% dispersant at a pH value of 10 is shown.

At the beginning of the measurement, the particle size distribution shows a bimodal size distribution with a d_{50} of 1.42 μm and a size variation from 0.04 μm to 9.82 μm. With increasing sedimentation time, the fraction of the coarser particles disappeared from the measurement field and the volume fraction of finer particles increases. After 53 h of sedimentation, the size distribution is still bimodal with a d_{50} decreased to 0.06 μm and a size variation from 0.04 μm to 0.31 μm. For each sedimentation time shown in Fig. 2, the maximum particle diameter can be determined and a settling velocity according to Stokes equation can be calculated. The sedimentation distance for particles measured by laser light diffraction is $s_1 = 25$ cm, the distance for particles measured by PIDS is $s_2 = 10$ cm. The velocity v of the particles can be calculated as follows:

$$v = \frac{s}{t} \tag{6}$$

The maximum particle diameters and the velocities calculated by using the Stokes equation and measured by laser light scattering and PIDS are shown in Fig. 3.

Depending on which measurement method is applied, sinking velocities for laser light scattering and PIDS are different. For particles with a diameter of 3.20 μm, the sinking velocity

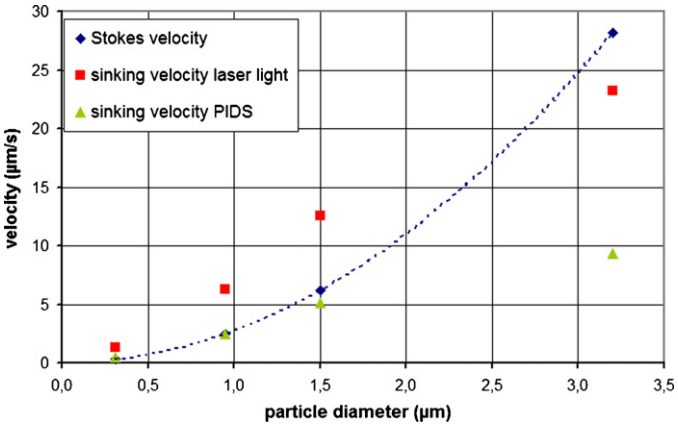

Fig. 3. Comparison of the velocities calculated and measured.

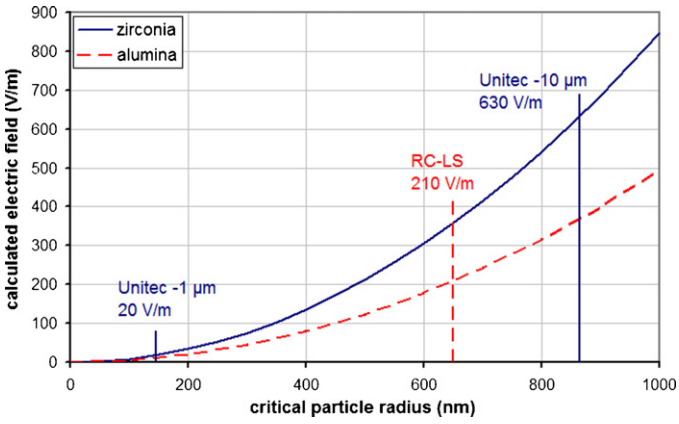

Fig. 4. Calculated critical electrical field strength.

measured in the chamber for laser light scattering is close to that calculated by using the Stokes equation. With decreasing particle size, the calculated velocities show different values. For particles with a diameter of 1.50 μm, the velocity measured in the sample chamber for PIDS approximates the velocity calculated by using the Stokes equation and are nearly equal for particles with a diameter of 0.95 μm. For the smallest particles with a diameter of 0.31 μm, the measured velocity is higher than the calculated velocity by using the Stokes equation. The difference for the intermediate particles with a diameter of 1.50 μm has to be explained by the measurement method. The particles are in the size area, where the two methods laser light scattering and PIDS overlap.

Thus the in situ measurement shows that the Stokes equation can be used very well for the mathematical description of the particle sinking velocities. Differences in measured and calculated velocities are referred to the real particle shape and to uncertainties of the measuring method.

3.3. Systematic interaction of sedimentation and electrical field in electrophoretic deposition

3.3.1. Fabrication of particle size gradients

For the mathematical description of S-EPD, kinetics of the electrophoretic deposition was analysed as reported previously.[29]

The results reported previously[29] indicate that Eq. (5) can be used for the calculation of the critical radius in S-EPD at least for stabilised aqueous suspensions with a solid content of 10 vol.%, because the kinetics of sedimentation and EPD can be described by the equations of Hamaker (Eq. (1)) and Stokes (Eq. (4)). Fig. 4 shows the required electrical field strength for different critical radii for the zirconia and alumina powders used in aqueous suspensions. The zeta potential ζ was −55 mV, the distance between the electrodes d was 15 mm. The r_{50} and the related critical electric field strength for the ZrO_2 and Al_2O_3 powders are highlighted for a better overview.

An aqueous slurry containing the Al_2O_3 powder RC-LS was made with a powder concentration of 10 vol.% and a dispersant concentration of 0.2 wt.%. The pH was adjusted to a value of 10. From this suspension a coating was electrophoretically deposited. The electric field was kept at 18 V/m for 10 min and then increased to a value of 36 V/m. After 5 min the field was further increased to 55 V/m and held constant for 5 min.

Fig. 5 shows the microstructure of the cross-sectional view of the deposit. The SEM picture above maps a scan across the deposit. First, a SEM picture of the electrode and the first electrophoretically deposited layer was taken, shown left on the image. On the right, the last deposited layer is shown.

For a better overview the first (left picture) and the last (right picture) deposited layers are shown at a higher magnification. It can be seen that close to the electrode rather fine particles are deposited. If the applied electrical field is increased, the size of the deposited particles increases.

Thus it can be demonstrated that by variation of the applied electrical field a fractionating respectively a systematic selection of the maximum deposited particle diameter can be achieved. The concentration of coarse particles deposited at 55 V/m is limited due to the particle size distribution of the RC-LS powder suspensions.

Thus for a pronounced effect of S-EPD an ideal powder should have a broad particle size distribution, possessing both nanoscaled particles and particles with a diameter of several 10 μm in comparable quantity. To obtain such a powder with identical properties, the Al_2O_3 powder RC-LS was calcined thereby creating coarse particles. This will be described in the following: the powder was heated with 10 K/min to a temperature of 1500 °C or 1550 °C, respectively in a chamber kiln (RHF 17/3E, Carbolite GmbH, Germany). The temperature was maintained for 10 h and then the furnace was cooled down to 30 °C with 10 K/min. The air flow rate was 5 l/min during the entire process. From the calcined powders aqueous suspensions with a solid content of 10 vol.% and a dispersant concentration of 0.2 wt.% were made and stabilised at pH 10 with TMAH. Particle size distributions of the two calcined powders and an identical suspension from the original powder are shown in Fig. 6.

Calcination of the powder at 1500 °C leads to a significant increase of the particle size in the suspension up to diameters of 33 μm compared to a maximum diameter of 4 μm of the original powder. While a further increase to 1550 °C only leads to a slight increase of the maximum particle diameter to 36 μm, the fraction of the coarse particles increases significantly.

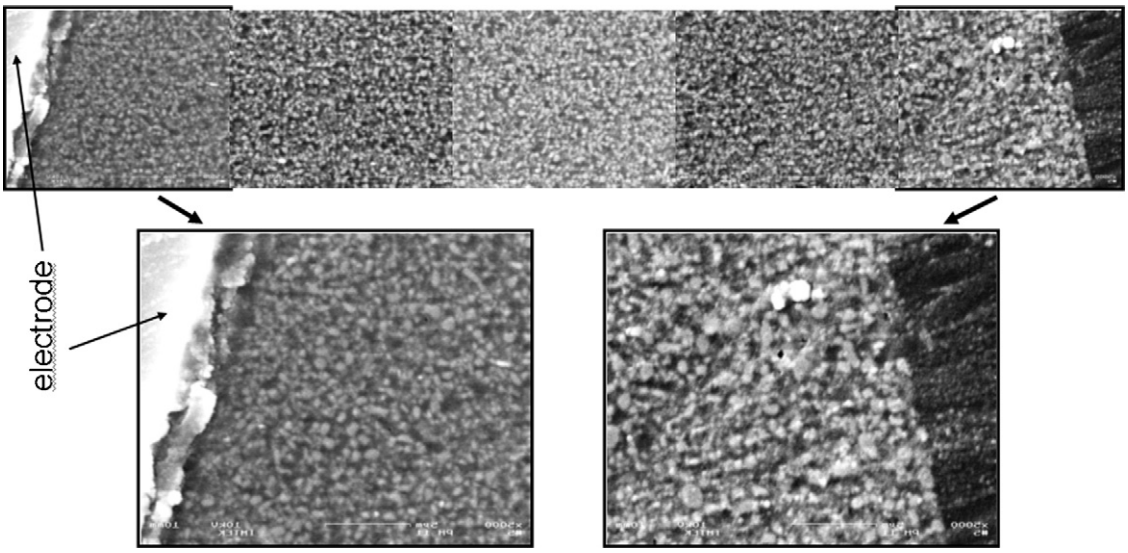

Fig. 5. SEM pictures of a layer consisting of Al_2O_3 powder RC-LS deposited by means of S-EPD..

From the 1550 °C calcined powder a suspension with ethyl alcohol as solvent was made and dispersed for 4 h at 200 min^{-1} in a planetary ball mill. The solid content was 30 vol.%, the dispersant (TODS) concentration was 2 wt.%. The solvent was evaporated and the powder was again calcined at 1550 °C. With this powder a similar suspension with a powder concentration of 20 vol.% was made and dispersed for 22 h in the ball mill. A larger quantity of the powder remained in the grinding beaker. These particles have not been dispersed and are thus not available for electrophoretic deposition. This is consistent with literature, whereby particles coarser than 30 μm cannot be used for electrophoretic deposition.[1,32] By weighing the powder surplus the powder concentration was calculated as 6 vol.%. Using ethyl alcohol allows the application of higher electrical fields because electrolysis compared to water starts only at higher applied voltages.

From this ethanolic suspension layers were electrophoretically deposited by means of S-EPD at different applied electrical fields for deposition times of 20 min. SEM pictures of the microstructure of the cross-section of the deposits respectively the particle size distribution were made and characterised. In Fig. 7 the deposits made at applied electrical fields of 333 V/m (left image), 1000 V/m (image in the center) and 2000 V/m (right image) are shown. It can be seen that the size of the deposited particles increases with the applied electrical field strength.

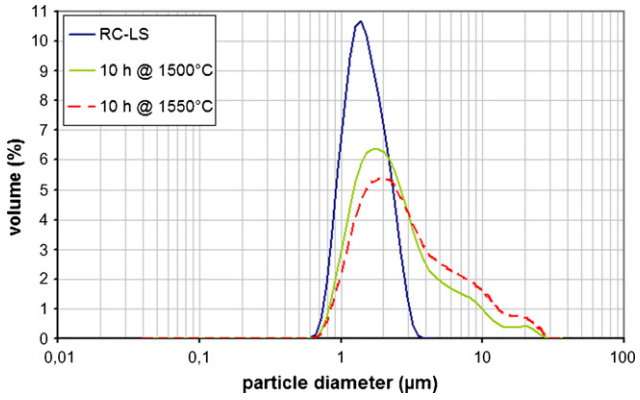

Fig. 6. Particle size distributions of the two calcined and the original powder.

3.3.2. *Fabrication of a compositional gradient (Al_2O_3–ZrO_2)*

An aqueous suspension with a powder concentration of 10 vol.% and a dispersant concentration of 0.3 wt.% was prepared and stabilised at a pH value of 10. The powder consisted of 60 wt.% of the "coarse" Al_2O_3 powder RC-LS and of 40 wt.% of the "fine" ZrO_2 powder Unitec – 1 μm. Due to electrolytical processes the maximum applied electrical field strength is limited to 200 V/m. Fig. 4 shows the calculated critical electric field strengths for the r_{50}-values of two ZrO_2 and one Al_2O_3 powder. It can be seen that the coarse ZrO_2-powder (Unitec – 10 μm) cannot be used because of its critical electrical field strength of 630 V/m.

Thus, with the suspension mentioned above a ZrO_2 gradient was deposited by S-EPD. An electrical field strength of 67 V/m was applied for 10 min and then it was gradually increased every 30 s by 6.7 V/m until after 10 min 200 V/m were reached. Before sintering the deposit was analysed concerning Al and Zr by using energy dispersive X-ray analysis. The Al and Zr content were analyzed at two positions: position 1 being close to the metal substrate, position 2 being close to the surface. From the measured Al and Zr fractions the Al_2O_3 and ZrO_2 composition can be calculated. At point "1" the ratio Al to Zr was measured as 0.70 ± 0.02, at point "2" as 0.83 ± 0.02. Translating Zr into ZrO_2 point "1" corresponds to a ZrO_2 fraction of 50.4 wt.%, point "2" corresponds to 46.3 wt.% ZrO_2.

In Figs. 8 and 9 the particle size distributions for the coarse Al_2O_3 powder RC-LS and the fine ZrO_2 powder Unitec – 1 μm are shown. Using equation (5) the critical radii for the two powders were calculated for electrical field strengths of 67 V/m and 200 V/m. The resultant critical diameters d_{crit} are highlighted for a better overview. For each applied electrical field strength

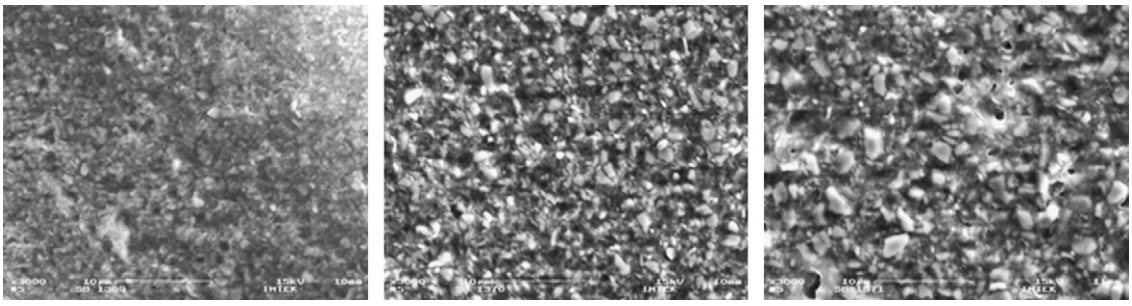

Fig. 7. SEM pictures of the deposits from the calcined powder.

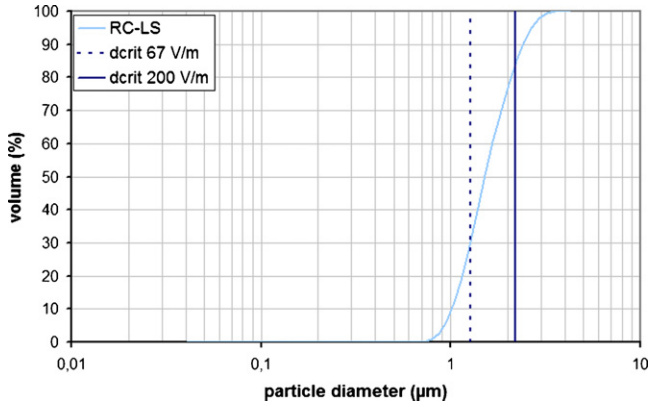

Fig. 8. Particle size distribution of the Al_2O_3 powder.

only the particle fraction left of the corresponding d_{crit}-line is taking part in electrophoretic deposition.

Thus for the Al_2O_3 powder for an electrical field strength of 67 V/m only 30% of the volume is taking part in EPD, while for 200 V/m 85% can be deposited. For the ZrO_2 powder for 67 V/m 92% of the volume is taking part in EPD, while for 200 V/m 99% can be deposited. Therefore for the given suspension at 67 V/m the calculated composition is 33 wt.% Al_2O_3 and 67 wt.% ZrO_2, for 200 V/m it is 56 wt.% Al_2O_3 and 44 wt.% ZrO_2. For increasing electrical field strengths the critical particle diameters and the compositions of Al_2O_3–ZrO_2 layers are calculated and shown in Fig. 10. Differences are due to the measurement method or the irregular form of the particles explained in Section 2.1. Also the discrepancy can be caused by the higher amount of small alumina particles available in the suspension as seen in particle size distribution due to the measurement method or disagglomeration during electrophoretic deposition. So more alumina particles will be deposited leading to a smaller zirconia amount than predicted.

It can be seen that from a suspension containing 60 wt.% Al_2O_3 and 40 wt.% ZrO_2 zirconia-rich layers can be electrodeposited at low electrical field strengths while with increasing electrical voltage the ZrO_2-content of the deposit decreases and approaches that of the suspension. Using Eq. (5) the critical radii for the two powders were calculated for different electrical field strengths. So for each applied electrical field strength from Figs. 8 and 9 the volume fraction taking part in EPD for Al_2O_3 and ZrO_2 can be read of. Using Eq. (2) and an assuming a constant green density of 50% from the deposited mass the resulting layer thickness is calculated for each applied electrical field strength. These discrete layer thicknesses are summed up to a cumulated layer thickness. Fig. 11 shows the calculated cumulated layer thickness of the discrete Al_2O_3–ZrO_2 layers deposited in 30 s at several electrical field strengths and the corresponding calculated ZrO_2 fraction. The two horizontal lines in Fig. 11 represent the measured ZrO_2-concentrations.

As the electrical field was increased by 6.7 V/m every 30 s the thickness of the deposited layer at each electrical voltage is increasing. This is due to two facts. Firstly if the green density of the deposit does not depend on the electric field according to Hamaker's law (Eq. (1)) the thickness of the layer deposited in a given time is proportional to the electrical field. Secondly as shown above in S-EPD the powder concentration taking part in

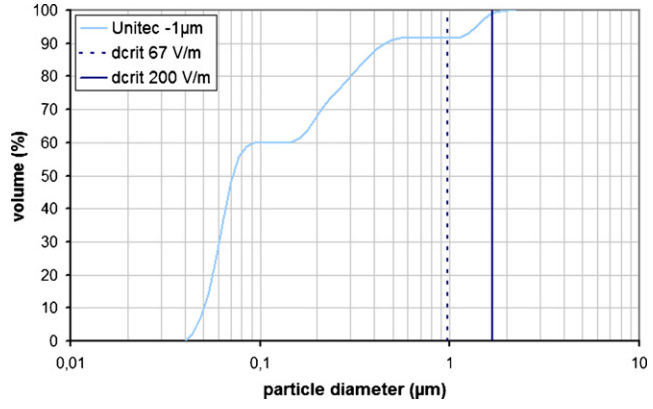

Fig. 9. Particle size distribution of the ZrO_2 powder.

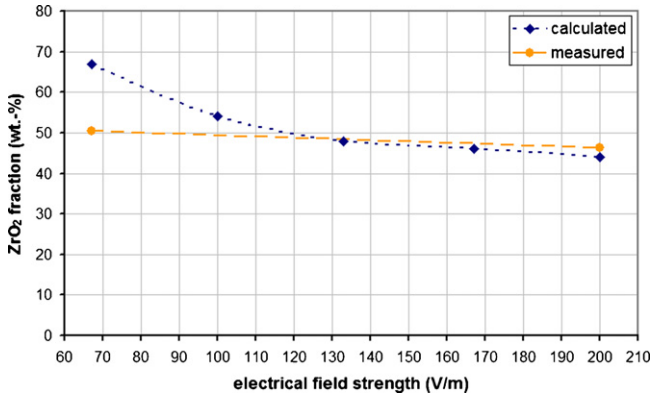

Fig. 10. Calcined and measured values of the ZrO_2 fraction.

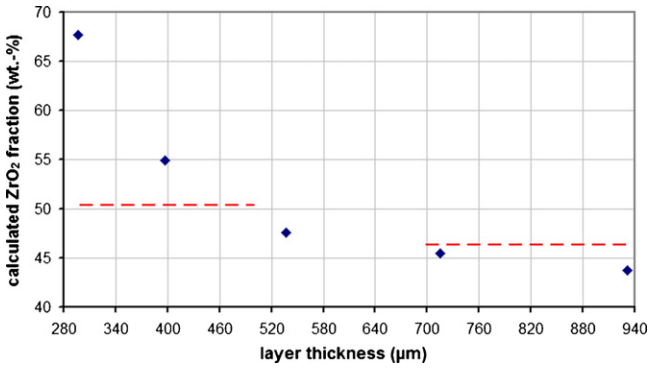

Fig. 11. Deposited layer thickness and the corresponding calculated ZrO_2 fraction.

electro-deposition is not constant but is increasing with increasing electric field. This is due to the fact, that only particles smaller than d_{crit} will be deposited. So with increasing electrical field d_{crit} the deposited volume fractions of both powders are increasing.

Both calculation and measurement show that the fraction of ZrO_2 is decreasing with increasing layer thickness, demonstrating that a compositional gradient can be achieved. The reasons for the obvious discrepancy between calculated and measured concentrations need to be further investigated. Especially the simplified assumption that the green density of the deposit is constant, independent of the electrical field strength and of the particle size distribution, requires further experiments. In addition it has to be considered that point "1" seems to be in the range of the layer deposited with increasing electrical field strength, thus r_{crit} is higher than used for calculation and so less ZrO_2 is deposited than predicted. At point "2" the deposition was not yet carried out with 200 V/m, so for the same reason more ZrO_2 is deposited and the measured ZrO_2 fraction is higher than predicted. Furthermore the calculated values represent the equilibrium state while the measured values represent transients because of the limited deposition times.

Eq. (1) shows the proportionality of the deposited mass and the electrical field strength. So with low applied electrical field strengths few mass and hence few particles are deposited resulting in a small deposited layer consisting of the smallest ZrO_2 and Al_2O_3 particles. Increasing the electrical field strength leads to the deposition of the coarse Al_2O_3 particles. Thus the deposited layers increases in size not only due to the higher applied electrical field strength resulting in higher deposited mass and hence in a thicker layer, but also due to the coarser Al_2O_3 particles in comparison with the layer composed of the fine particles. So consequentially due to the measurement method with a high probability not only the first deposited layers are characterised but also the adjoining layers deposited with higher electrical field strength resulting in a lower ZrO_2 fraction than expected.

4. Conclusions

It was shown that the experimentally determined kinetics of sedimentation can be described by Stokes' equation. Also, the kinetics of electrophoretic deposition and S-EPD can both be very well described by Hamaker's equation as reported previously.[29] The functionality of S-EPD was demonstrated. Gradients in particle size distribution in the electrophoretically deposited layer as a function of the applied electrical field could be observed.

It could also be demonstrated, that the zeta potential of the used zirconia and alumina suspensions are nearly identical in basic pH range. First experiments show that simultaneous deposition of zirconia and alumina is possible and that with zirconia and alumina powders with suitable particle size distributions a compositional gradient can be achieved when the electrical field is changed during S-EPD.

Acknowledgement

Our sincere thanks go to all colleagues for their support and encouragement.

References

1. Boccaccini, A. R. and Zhitomirsky, I., Application of electrophoretic and electrolytic deposition techniques in ceramics processing. *Curr. Opin. Solid State Mater. Sci.*, 2002, **6**, S.251–S.260.
2. Harbach, F. and Nienburg, H., Homogeneous Functional ceramic components through electrophoretic deposition from stable colloidal suspensions. I. Basic concepts and applications to zirconia. *J. Eur. Ceram. Soc.*, 1998, **18**(6), S.675–S.683.
3. Reuss, F. F., Notice sur un nouvel effet de l'électricité galvanique. *Mémoires de la Societé Impériale des Naturalistes de Moscou*, 1808, S.327–S.337.
4. Hamaker, H. C., Formation of deposit by electrophoresis. *Trans. Faraday Soc.*, 1940, **36**, S.279–S.287.
5. Van Der Biest, O. O. and Vandeperre, L. J., Electrophoretic deposition of materials. *Annu. Rev. Mater. Sci.*, 1999, **29**, S.327–S.352.
6. Tabellion, J. and Clasen, R., Electrophoretic deposition from aqueous suspensions for near-shape manufacturing of advanced ceramics and glasses-applications. *J. Mater. Sci.*, 2004, **39**, S.803–S.811.
7. Sarkar, P., Datta, S. and Nicholson, P. S., Functionally graded ceramic/ceramic and metal/ceramic composites by electrophoretic deposition. *Compos. Part B-Eng.*, 1997, **28**(1–2), S.49–S.56.
8. Nagarajan, N. and Nicholson, P. S., Nickel-alumina functionally graded materials by electrophoretic deposition. *J. Am. Ceram. Soc.*, 2004, **87**(11), S.2053–S.2057.
9. Oetzel, C., Clasen, R. and Tabellion, J., Electric field assisted processing of ceramics. *cfi-Ceram. Forum Int.*, 2004, **81**, S.35–S.41.
10. Biesheuvel, P. M. and Verweij, H., Theory of cast formation in electrophoretic deposition. *J. Am. Ceram. Soc.*, 1999, **82**(6), S.1451–S.1455.
11. Simovic, K., Miskovic-Stankovic, V. B., Kicevic, D. and Jovanic, P., Electrophoretic deposition of thin alumina films from water suspensions. *Colloid. Surf. A*, 2002, **209**, S.47–S.55.
12. Sarkar, P. and Nicholson, P. S., Electrophoretic deposition (EPD): mechanism, kinetics and application to ceramics. *J. Am. Ceram. Soc.*, 1996, **79**, S.1987–S.2002.
13. Sarkar, P., Huang, X. and Nicholson, P. S., Zirconia/alumina functionally gradiented composites by electrophoretic deposition techniques. *J. Am. Ceram. Soc.*, 1993, **76**, S.1055–S.1056.
14. Kaya, C., Al_2O_3-Y-TZP/Al_2O_3 functionally graded composites of tubular shape from nano-sols using double-step electrophoretic deposition. *J. Eur. Ceram. Soc.*, 2003, **23**(10), S.1655–S.1660.
15. Ferrari, B., Sánchez-Herencia, A. J. and Moreno, R., Electrophoretic forming of Al_2O_3/Y-TZP layered ceramics from aqueous suspensions. *Mater. Res. Bull.*, 1998, **33**(3), S.487–S.499.
16. Hadraba, H., Maca, K. and Cihlar, J., Electrophoretic deposition of alumina and zirconia. II. Two-component systems. *Ceram. Int.*, 2004, **30**(6), S.853–S.863.

17. Put, S., Anné, G., Vleugels, J. and Van der Biest, O., Advanced symmetrically graded ceramic and ceramic–metal composites. *J. Mater. Sci.*, 2004, **39**(3), S.881–S.888.
18. Batchelor, G. K., Sedimentation in a dilute dispersion of spheres. *J. Fluid Mechan.*, 1972, **52**, S.245–S.268.
19. Dushkin, C., Miwa, T. and Nagayama, K., Gravity effect on the field deposition of two-dimensional particle arrays. *Chem. Phys. Lett.*, 1998, **285**(3–4), S.259–S.265.
20. Avgustinik, A. I., Vigdergauz, V. S. and Zhuravlev, G. I., Electrophoretic deposition of ceramic masses from suspensions and calculation of deposit yields. *Zh. Prikl. Khim.*, 1962, **35**(10), S.2090–S.2093.
21. Avgustinik, A. I., Zhuravlev, G. I. and Vigdergauz, V. S., Calculation of the yield of deposit in electrophoretic deposition. *J. Appl. Chem. USSR*, 1966, **35**(10), S.379–S.383.
22. Tabellion, J., Herstellung von Kieselgläsern mittels elektrophoretischer Abscheidung und Sinterung. Dissertation, Universität des Saarlandes, (2004), 213 Seiten.
23. Zhang, Z. T., Huang, Y. and Jiang, Z. Z., Electrophoretic deposition forming of SiC-TZP composites in a nonaqueous sol media. *J. Am. Ceram. Soc.*, 1994, **77**(7), S.1946–S.1949.
24. Kynch, G. J., A theory of sedimentation. *Trans. Faraday Soc.*, 1952, **48**(2), S.166–S.176.
25. Bürger, R. and Wendland, W. L., Sedimentation and suspension flows: historical perspective and some recent developments. *J. Eng. Math.*, 2001, **41**, S.101–S.116.
26. Barreiros, F. M., Ferreira, P. J. and Figueiredo, M. M., Calculating shape factors from particle sizing data. *Partic. Partic. Syst. Charact.*, 1996, **13**(6), S.368–S.373.
27. Lehmann, M., Berthold, C., Pabst, W., Gregorová, E. and Nickel, K. G., Particle size and shape characterization of kaolins—comparison of settling methods and laser diffraction. *Key Eng. Mater.*, 2004, **264–268**, S.1387–S.1390.
28. Bonnas, S., Tabellion, J. and Hausselt, J., Effect of particle size distribution and sedimentation behaviour on electrophoretic deposition of ceramic suspensions. *Key Eng. Mater.*, 2006, **314**, S.69–S.74.
29. Bonnas, S., Tabellion, J., Ritzhaupt-Kleissl, H. J. and Haußelt, J., Systematic interaction of sedimentation and electrical field in electrophoretic deposition. In *Second International Conference on Multi-Material Micro Manufacture*, ed. W. Menz, S. Dimov and B. Fillon. Elsevier, 2006.
30. Wildhack, S., *Herstellung flüssigphasengesinterter Schichtkomposite aus SiC und AlN*. Doktor, Universität Stuttgart, 2003, 127 Seiten.
31. Yang, M., Neubauer, C. M. and Jennings, H. M., Interparticle potential and sedimentation behavior of cement suspensions—review and results from paste. *Adv. Cement Mater.*, 1997, **5**(1), S.1–S.7.
32. Heavens, S. N., Electrophoretic deposition as a processing route for ceramics. In *Advanced Ceramic Processing and Technology*, ed. J. G. P. Binner. Noyes Publication, Park Ridge, NJ, 1990, pp. S.255–S.283.